

# Robust $\mu$ -synthesis controllers for suppressing stick-slip induced vibrations in oil well drill strings

M. Karkoub · M. Zribi · L. Elchaar · L. Lamont

Received: 12 April 2008 / Accepted: 24 September 2009 / Published online: 6 November 2009  
© Springer Science+Business Media B.V. 2009

**Abstract** Stick-slip friction is a major cause of drill-string failure. This paper addresses the problem of suppressing stick-slip induced oscillations in oil well drill strings using a control design technique known as  $\mu$ -synthesis. This technique allows for the inclusion of modeling errors in the control design process in terms of uncertainty weights. The dynamic model of the drill string with stick-slip friction is highly nonlinear and has to be linearized around an operating point in order to use  $\mu$ -synthesis. The difference between the linear and nonlinear models is characterized in terms of uncertainty weights and included in the control design process. The designed controllers are robust to uncertainty in the dynamic model, spillover, actuator uncertainty, and noise. Two controllers were designed using  $\mu$ -synthesis and the simulation results are presented and discussed here. The first controller assumes no measurement delay; however, the second controller includes a sensor time delay in the measurements. Both controllers are robust and performed well.

**Keywords** Drill string · Robust control ·  $\mu$ -synthesis · Time delay system

## 1 Introduction

The drilling process is affected by the dynamically induced vibrations due to design imperfections as well as material elasticity. Vibrations can decrease the rate of penetration (ROP) and thereby increase the cost of the well and can interfere with measurement-while-drilling (MWD) tools [18, 21]. There have been a significant number of research publications on drill-string dynamics and a representative few are considered in this paper. Several models

---

M. Karkoub (✉)

Department of Mechanical Engineering, Texas A&M University, P.O. Box 23874, Doha, Qatar  
e-mail: [mkarkoub@pi.ac.ae](mailto:mkarkoub@pi.ac.ae)

M. Zribi

Department of Electrical Engineering, Kuwait University, P.O. Box 5969, Safat 13060, Kuwait

L. Elchaar · L. Lamont

Department of Electrical Engineering, The Petroleum Institute, Abu Dhabi, United Arab Emirates

are available in the literature which include one or more of the following phenomena: bit bounce, stick-slip, forward and backward whirl, axial, lateral, and torsional vibrations. The torsional vibrations of a drill string can lead to excessive loadings resulting in equipment wear, joint failure, or damage of the drill-bit [5]. It has been verified through downhole measurements that the application of a constant rotary speed at the surface does not necessarily translate into a constant speed rotation of the drill-bit. This discrepancy in the rotational speed of the drill string is due to the large torsional flexibility of the drilling assembly. The rig floor can experience significant dynamic torque fluctuation because of the torsional vibrations. One major cause of torsional vibrations is the stick-slip friction. Stick-slip is a self-excited torsional vibration induced by the nonlinear relationship between the friction-induced torque and the angular velocity at the bit [11]. Since the early eighties, the stick-slip phenomenon has been extensively examined both analytically and experimentally; see for example [6, 11, 13–17, 20, 22]. The available models range from simple ones based on lumped mass theory to more complex models which make use of the elasticity theory coupled with some modeling technique such as finite elements and the Hamiltonian principle; see for example [7, 8, 13–15, 23].

A lot of research has been focused on minimizing the effect of the torsional vibrations. For example, one technique introduced in the 1980s used an active damping system to resolve the problem of stick-slip in drill strings. This system reduces the torque fluctuations and torsional drill-string vibrations affecting in this manner the stick-slip conditions. Torque feedback is used to reduce the amplitude of the downhole rotational vibrations by automatically slowing down or increasing the rotary rate depending on whether the torque is increasing or decreasing; see for example [10, 11, 20, 22, 23]. Many control techniques have been used in the past decade or so: Serrarens et al. [19] used  $H_\infty$  control in suppressing stick-slip oscillations whereas Christoforou and Yigit [8] used state feedback control. Hiddabi et al. [3] developed a nonlinear controller to reduce the vibration oscillations. The control law is based on input–output linearization and the authors showed, through simulations, the effectiveness of the control law. Abdulgalil and Siguerdidjane [1, 2] developed a PID and backstepping controllers to reduce the effect of the torsional vibrations. The PID controller is used in conjunction with a state input controller because of the uncertainties in the system.

It is worth mentioning that the drill-string dynamic model is underactuated since the system has two degrees of freedom and only one torque is used to control the action of the system. One control technique which has been used successfully in the control of underactuated systems is  $\mu$ -synthesis [4, 9, 12]. This technique is based on  $H_\infty$  control design and an optimization technique known as D-K iterations. The advantage of this technique is that it allows the inclusion of modeling imperfections in the control design process. Once designed, the controller will be robust to all uncertainties included as long as the  $\mu$  values are less than 1 for all frequencies.

In this paper, a 3rd order model of the drill-string system is used with the states being the speeds of the rotary table and the drill collar and the twist angle of the drill pipe. The model is nonlinear and includes the effect of the stick-slip friction. A linear model is derived and used as the nominal plant for the control design process. The difference between the actual model and the linearized one are characterized in terms of uncertainty weights and included in the closed-loop system. Moreover, noise and actuator uncertainties are also included in the closed-loop system. The designed controllers are robust to high-frequency dynamics, modeling errors, actuator uncertainty and noise. Another issue that is addressed here is the location of the sensors. Due to the fact that the rotary table and the drill collar could be miles apart, time delay in the measurement might cause problems while doing real time control. Therefore, another controller is designed assuming a time delay in the measurements.

The rest of the paper is organized as follows: A dynamic model for the drill string is presented in Sect. 2. The  $\mu$ -synthesis control design weights are selected in Sect. 3. The  $\mu$ -synthesis controller design results are discussed in Sect. 4. Finally, some concluding remarks are listed in Sect. 5.

## 2 Dynamic model of the drill-string system

Consider the drilling system represented in Fig. 1.

Let,

- $\phi_1$ : angular displacement of the bit
- $\phi_2$ : angular displacement of the rotary table
- $\phi$ : difference between  $\phi_2$  and  $\phi_1$  ( $\phi = \phi_2 - \phi_1$ )
- $\Omega_1$ : angular speed of the bit, ( $\Omega_1 = \dot{\phi}_1$ )
- $\Omega_2$ : angular speed of the rotary table, ( $\Omega_2 = \dot{\phi}_2$ )
- $\Omega_{ref}$ : desired angular speed of the bit
- $J_1$ : equivalent moment of inertia of the collars and the drill pipes
- $J_2$ : inertia of the rotary table augmented with inertia of the electric motor ( $J_2 = J_{table} + n^2 J_m$ )
- $J_{table}$ : moment of inertia of the rotary table
- $J_m$ : moment of inertia of the electric motor
- $n$ : transmission gear box ratio
- $C_1$ : equivalent viscous damping coefficient of the bottom hole assembly (BHA)
- $C_2$ : viscous damping of the rotary table

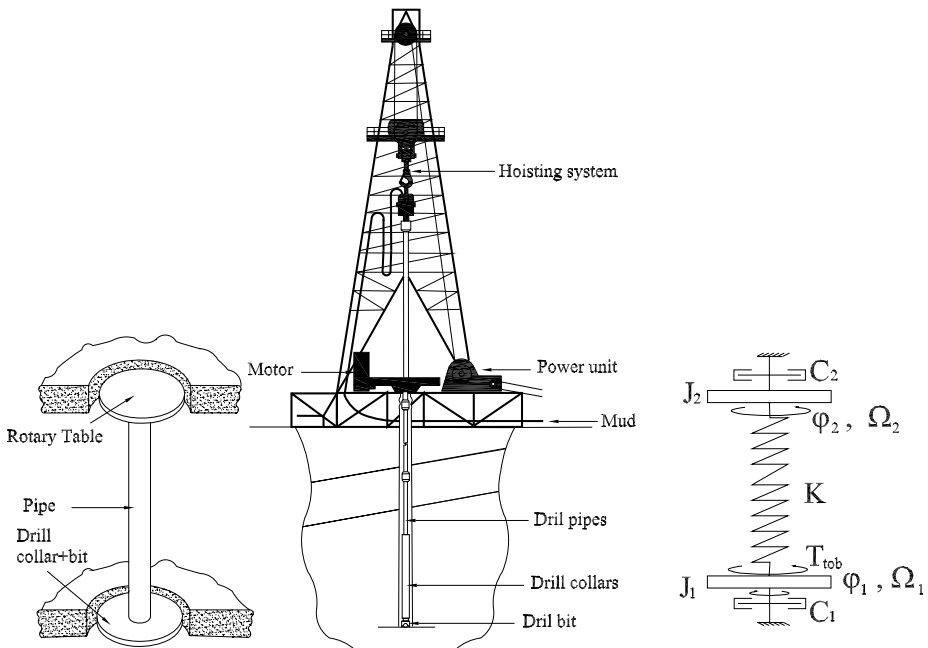


**Fig. 1** Schematic diagram of a drill string

- $T_1$ : torque on bit
- $T_2$ : torque delivered by the motor

The equations of motion of the drill-string system are as follows [19]:

$$\begin{aligned}
 J_1\dot{\Omega}_1 + C_1\Omega_1 - K\phi &= -T_1(\Omega_1) \\
 \dot{\phi} &= \Omega_2 - \Omega_1 \\
 J_2\dot{\Omega}_2 + K\phi + C_2\Omega_2 &= T_2
 \end{aligned}
 \tag{1}$$

where

$$T_1(\Omega_1) = T_t \frac{2}{\pi} (\alpha_1 \Omega_1 e^{-\alpha_1 |\Omega_1|} + \text{atan}(\beta \Omega_1)) \tag{2}$$

$$T_2 = u \tag{3}$$

Note that the torque  $T_1(\Omega_1)$  in (2) is taken from reference [19] where  $T_t$ ,  $\alpha_1$ ,  $\alpha$  and  $\beta$  are given scalars.

Combining equations (1) and (3), the dynamic model of the system can be written as

$$\begin{aligned}
 \dot{\Omega}_1 &= -\frac{C_1}{J_1}\Omega_1 + \frac{K}{J_1}\phi - \frac{1}{J_1}T_1(\Omega_1) \\
 \dot{\phi} &= \Omega_2 - \Omega_1 \\
 \dot{\Omega}_2 &= -\frac{K}{J_2}\phi - \frac{C_2}{J_2}\Omega_2 + \frac{1}{J_2}u
 \end{aligned}
 \tag{4}$$

Let the parameters of the system be such that  $p_1 = -\frac{C_1}{J_1}$ ,  $p_2 = \frac{K}{J_1}$ ,  $p_3 = -\frac{2}{J_1\pi}\alpha_1 T_t$ ,  $p_4 = -\frac{2}{J_1\pi}T_t$ ,  $p_5 = -\frac{K}{J_2}$ ,  $p_6 = -\frac{C_2}{J_2}$ , and  $p_7 = \frac{1}{J_2}$ .

Also, let the states of the system be such that  $x_1 = \Omega_1$ ,  $x_2 = \phi$  and  $x_3 = \Omega_2$  with  $X = [x_1 \ x_2 \ x_3]^T$ .

Using these parameters, the model of the system (4) can be written as

$$\begin{aligned}
 \dot{x}_1 &= p_1x_1 + p_2x_2 + p_3x_1e^{-\alpha_1|x_1|} + p_4\text{atan}(\beta x_1) \\
 \dot{x}_2 &= -x_1 + x_3 \\
 \dot{x}_3 &= p_5x_2 + p_6x_3 + p_7u
 \end{aligned}
 \tag{5}$$

The model can be written in the following form:

$$P = P_{\text{nom}} + \Delta W \tag{6}$$

where  $P_{\text{nom}}$  is the linearized version of (5) and given by

$$\dot{X} = [A]X + [B]u \tag{7}$$

and  $\Delta W$  is an uncertainty function that will account for the difference between the actual plant and the nominal one. Therefore, a good robust control technique, such as  $\mu$ -synthesis, could be used to design controllers to reduce the effect of stick-slip and other modeling uncertainties. The  $\mu$ -synthesis technique is an  $H_\infty$  based control design which allows for the integration of modeling errors as weighting function. Following is a brief overview of the technique.

### 3 $\mu$ -Synthesis controller design

The  $H_\infty/\mu$ -synthesis control technique is used here to synthesize a controller for the drill-string system. The designed controller has to be insensitive to unmodeled high frequency dynamics, neglected nonlinearities and variations in the drill-string assembly material properties. To better understand the proposed control scheme, a brief description of the  $\mu$  technique will be given here. The reader can refer to [4, 9] for more details on the  $\mu$ -synthesis control design.

Let  $P$  be an  $n \times n$  complex matrix,  $P \in \mathbf{C}^{n \times n}$ , which represents a nominal closed-loop system; let  $S$  and  $F$  be integers such that  $S, F > 0$  and  $r_1, r_2, \dots, r_S$  and  $m_1, m_2, \dots, m_F$  be positive integers such that

$$\sum_{i=1}^S r_i + \sum_{j=1}^F m_j = n \tag{8}$$

Let  $\Delta$  be the uncertainty matrix associated with the nominal closed-loop system  $P$  and  $\mathbf{\Delta}$  be the set of block diagonal matrices in  $\mathbf{C}^{n \times n}$  with  $S$  scalar blocks and  $F$  full blocks such that

$$\mathbf{\Delta} = \left\{ \begin{array}{l} \text{diag}[\delta_1 I_{r_1}, \dots, \delta_S I_{r_S}, \Delta_1, \dots, \Delta_F] \\ \delta_i \in \mathbf{C}, \Delta_j \in \mathbf{C}^{m_j \times m_j} \end{array} \right\} \tag{9}$$

and

$$B_{\mathbf{\Delta}} = \{ \Delta \in \mathbf{\Delta} : \bar{\sigma}(\Delta) \leq 1 \} \tag{10}$$

A permissible  $\Delta$  in  $B_{\mathbf{\Delta}}$ , destabilizes the closed-loop system  $(P, \Delta)$  if and only if

$$\det[I - P(j\omega)\Delta(j\omega)] = 0 \tag{11}$$

The Structured Singular Value Function (known as  $\mu$ ) is defined as follows:

$$\mu(P(j\omega)) = \begin{cases} [\min_{\Delta \in B_{\mathbf{\Delta}}} \bar{\sigma}(\Delta(j\omega)) : \det(I - P\Delta) = 0]^{-1} & \text{otherwise,} \\ 0 & \text{if } \det[I - P(j\omega)\Delta(j\omega)] \neq 0 \forall \Delta \in B_{\mathbf{\Delta}} \end{cases} \tag{12}$$

where  $\bar{\sigma}$  denotes the maximum singular value [9].

It can be shown that for the feedback system to remain stable for all stable and bounded  $\Delta$ 's,  $\mu$  has to be less than 1 over all frequencies ([4] and [9]):

$$\sup_{\omega} \mu(P(j\omega)) \leq 1 \tag{13}$$

For computation purposes, it was shown by Doyle [9] that

$$\rho(P) \leq \mu(P) \leq \bar{\sigma}(P) \tag{14}$$

However, since the difference between the spectral radius,  $\rho$ , and the maximum singular value,  $\bar{\sigma}$ , can be arbitrarily large, better estimates of the lower and upper bounds of  $\mu$  should be obtained. The  $\mu$ -synthesis technique makes use of a minimization scheme known as ‘‘D–K iteration’’ to obtain less conservative bounds on the  $\mu$  values across the frequency spectrum. D–K iteration is basically a two-step minimization process: the first step is a minimization over all stabilizing controllers  $K$  while a scaling matrix  $D$  is held fixed, and the second step is a minimization over the scaling matrix  $D$  while the controller  $K$  is kept fixed.

### 3.1 Additive and multiplicative uncertainty description

A control design block diagram is shown in Fig. 2. Two forms of modeling uncertainty can be included in the closed-loop formulation using the  $H_\infty$  control design technique: additive and input multiplicative. The additive uncertainty weighting matrix,  $[W_a]$  in the drill-string system block diagram (see Fig. 2), represents the unmodeled dynamics of the system and it is selected such that  $[W_a]$  is low in magnitude at low frequency and high at high frequency. This is reasonable since at low frequencies, the dynamic model is fairly accurate. At high frequencies, unmodeled dynamics and nonlinearities may have a tremendous impact on the behavior of the system. Moreover,  $[W_a]$  limits the bandwidth of the system and enforces a roll-off constraint on the closed-loop system. The additive uncertainty weighting matrix is selected such that

$$\begin{bmatrix} \frac{111s+2.5}{s+62} & 0 & 0 \\ 0 & \frac{111s+2.5}{s+62} & 0 \\ 0 & 0 & \frac{111s+2.5}{s+62} \end{bmatrix} \tag{15}$$

This indicates that the drill-string system could vary by as much as 5% at low freq and increases gradually to reach 100% at 100 rad/sec. The other type of uncertainty that will be included in the control design is input multiplicative. The input uncertainty weight,  $W_{act}$ , shown in Fig. 2, is included in the control problem formulation to account for input modeling errors and uncertainties of the linearized actuator model. The actuator uncertainty weight is selected such that

$$W_{act} = \frac{1.1s + 55}{s + 2000} \tag{16}$$

This weight implies that there is approximately 2.5% error in the input signal at low frequency which rises up to 90% at high frequency. The multiplicative input uncertainty weight helps limit the bandwidth of the system, while increasing the system robustness to changes in the plant model. Although variations in the drill-string assembly parameters have not been directly accounted for in the control design model, both the additive and multiplicative uncertainty weights have been designed with robustness to these variations in mind.

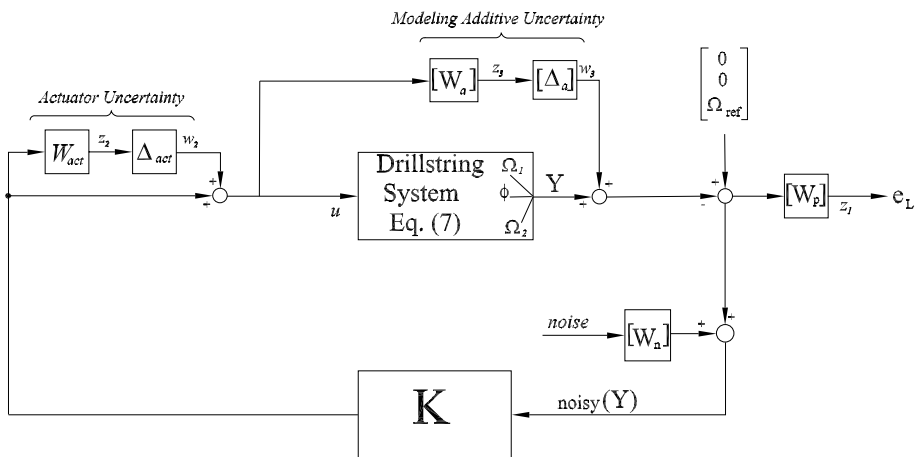


**Fig. 2** Block diagram of the closed-loop system for the  $\mu$ -synthesis control design

### 3.2 Measurement noise

The interconnection diagram in Fig. 2 shows the weighting noise matrix  $[W_n]$ .  $[W_n]$  is a frequency varying matrix used to model the magnitude of the sensor’s noise in the measurement of the rotational speeds of the rotary table and the drill collar. The transfer matrix is selected such that

$$[W_n] = \begin{bmatrix} \frac{0.125(s+1)}{s+100} & 0 & 0 \\ 0 & 0 & 0 \\ 0 & 0 & \frac{0.125(s+1)}{s+100} \end{bmatrix} \tag{17}$$

which corresponds to the noise level in the measurement sensor channels. This weighting matrix indicates that the level of noise is low at low frequencies ( $1.25 \times 10^{-3}$ ) and increases to 0.125 at frequencies.

### 3.3 Time delay uncertainty

Since the distance between the drill collar and the controller could be in the kilometers range, there is usually a delay in transmitting the signal to the surface. Therefore, the dynamics of the drill-string system will include a time delay due to the sensors location. It is desired to transform this transport lag to a system uncertainty which can be easily integrated in the closed-loop model. The closed-loop system is shown in Fig. 3 in which the system time delay due to the location of the sensor is cascaded with the drill-string system transfer function. The sensor time delay is taken as

$$\tau_d = 2 \text{ sec} \tag{18}$$

The control diagram in Fig. 3 can be reconfigured to reflect the time delay in the dynamics of the system as a perturbation. Therefore, if one chooses a perturbation  $\Delta_\tau(s)$  such that

$$\Delta_\tau(s) = e^{-\tau_d s} - 1 \tag{19}$$

then, the closed-loop diagram can be transformed as shown in Fig. 4. However, care has to be taken with this choice of perturbation since its infinity norm is equal to 2; that is,

$$\|\Delta_\tau\|_\infty = \|e^{-\tau_d s} - 1\|_\infty = 2 \tag{20}$$

For the closed-loop system to achieve robust performance, the designed controller must be robust to the time delay and all other perturbations of magnitude 2. However, this will limit

**Fig. 3** Block diagram of the closed-loop system with measurement time delay

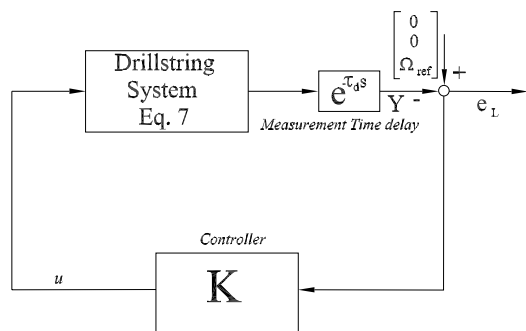


**Fig. 4** Block diagram of the closed-loop system with time delay as output multiplicative uncertainty

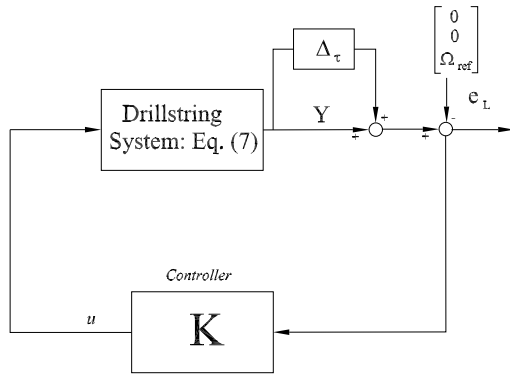
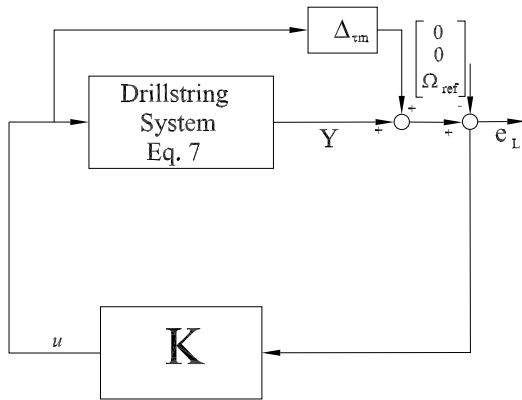


**Fig. 5** Block diagram of the closed-loop system with time delay as additive uncertainty



the choices of controllers and make the control law unnecessarily conservative. In order to use the  $\mu$ -synthesis technique, all perturbations must be less than 1 in magnitude. Therefore, a variable change will be made so that the perturbation satisfies the magnitude less than 1 requirement. The perturbation  $\Delta_\tau(s)$  is small at low frequencies and grows large at high frequencies. That is

$$\lim_{s \rightarrow 0} \Delta_\tau(s) = 0 \quad \text{and} \quad \lim_{s \rightarrow \infty} \Delta_\tau(s) = 2 \tag{21}$$

Therefore, one can include this perturbation as an additive uncertainty surrounding the drill-string system as shown in Fig. 5. The new perturbation  $\Delta_{\tau m}$  is given by

$$\Delta_{\tau m}(s) = \Delta_\tau P \tag{22}$$

where  $P$  represents the linearized drill-string assembly dynamics given by (7) assuming that the maximum time delay is 2 seconds. Since each transfer function of  $P$  is strictly proper, there is a single input single output bandpass filter  $w_d(s)$  such that

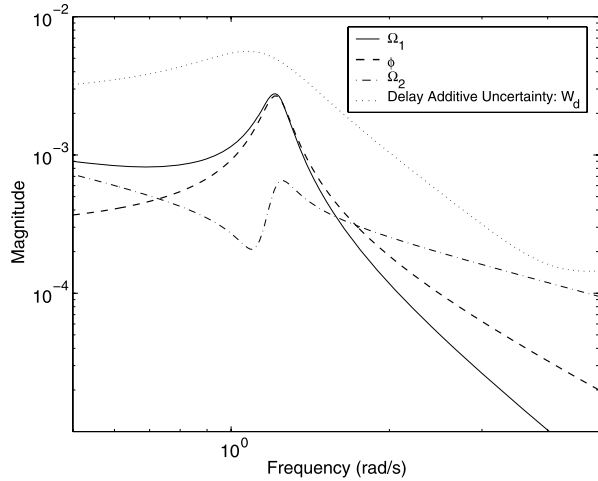
$$\|w_d^{-1} \Delta_{\tau m}\|_\infty < 1 \tag{23}$$

The weighting function is chosen such that

$$|W_d(j\omega)| > |\Delta_\tau(j\omega)P(j\omega)| \quad \forall \tau \leq 2 \text{ sec and } \forall \omega \tag{24}$$



**Fig. 6** Weighting function for time delay replacement



The transfer matrix  $W_d$  is selected such that

$$[W_d] = \begin{bmatrix} w_d & 0 & 0 \\ 0 & 0 & 0 \\ 0 & 0 & w_d \end{bmatrix} \begin{bmatrix} \frac{2s^2+6s+36}{s^2+0.5s+1.3} & 0 & 0 \\ 0 & 0 & 0 \\ 0 & 0 & \frac{2s^2+6s+36}{s^2+0.5s+1.3} \end{bmatrix} \tag{25}$$

Figures 2, 3, 4, 5 and 6 shows a plot of  $|\Delta_\tau(j\omega)P(j\omega)|$  as a function of frequency as well as the selected weighting transfer function  $w_d$  to show that inequality 24 holds for all frequencies.

### 3.4 Performance description

The  $\mu$ -synthesis design technique requires all performance and robustness specifications be described as weighting functions on the system transfer functions. These weighting functions serve two purposes in the  $H_\infty$  framework: they not only allow the direct comparison of different performance objectives with the same norm, but also allow frequency information to be incorporated into the analysis. The desired  $\Omega_{ref}$   $Y$  response of the drill-string system is formulated as a model matching problem in the  $\mu$  framework (see Fig. 2). The differences between the input command  $\Omega_{ref}$  and the drill-string assembly rotational speeds  $Y$  are used to generate an error  $e_L$  to be minimized for robust performance. Therefore, the performance weight must be selected in a manner that will make it possible to design a robust controller for the drill-string system. A performance weight has been prescribed requiring a disturbance rejection at low frequency to be of the order of 100-to-1. This also means that the steady-state tracking error for the lateral displacement should be in the order of 0.01 or smaller. This requirement is relaxed as the frequency increases and up to 0.6 rad/s, the closed-loop system will perform better than the open-loop one. The closed-loop performance will decrease with frequency, but it will always lie underneath the envelope traced by the inverse of the performance weight to guarantee robustness.

### 3.5 Controller design

The first controller is designed based on the control diagram shown in Fig. 2. The block diagram could be rearranged to look like Fig. 7 where the perturbation block,  $\Delta$  includes

**Fig. 7** Block diagram of the closed-loop system for the  $\mu$ -synthesis control design

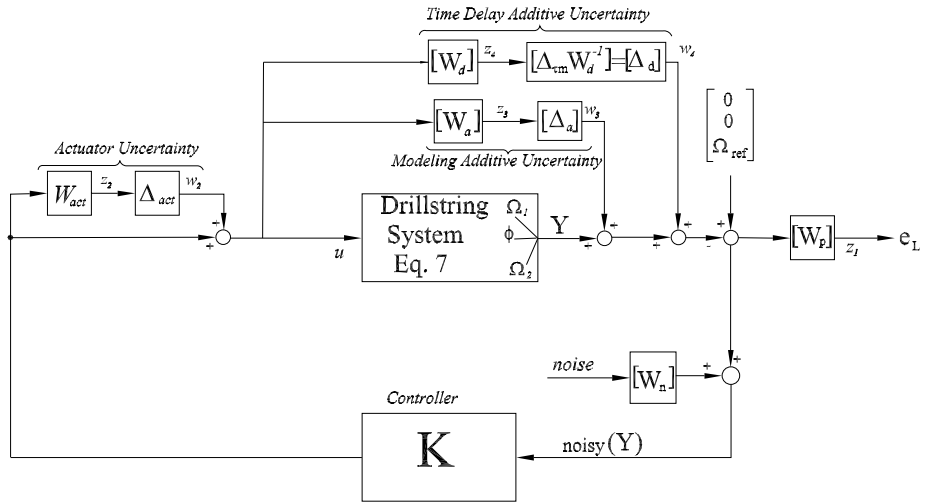
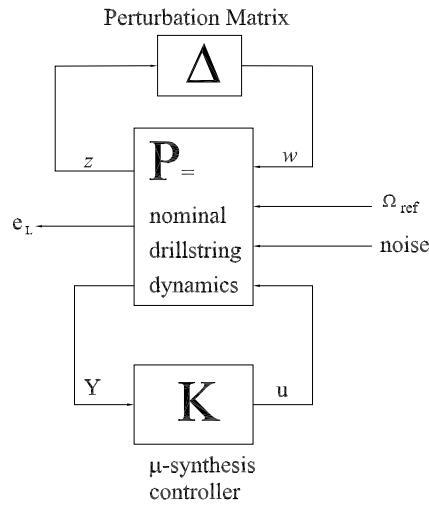


**Fig. 8** Control design block diagram for the drill string system with measurement time delay for the  $\mu$ -synthesis control design

the performance uncertainty block,  $[\Delta_p]$ , the actuation uncertainty block  $\Delta_{act}$ , and additive uncertainty due modeling errors,  $[\Delta_a]$ . The uncertainty block  $\Delta$  is given by

$$\Delta = \begin{bmatrix} [\Delta_p] & 0 & 0 \\ 0 & \Delta_{act} & 0 \\ 0 & 0 & [\Delta_a] \end{bmatrix} \tag{26}$$

For the case where measurement time delay is included in the closed-loop system, the control design block diagram is shown in Fig. 8. As before, the block diagram can be rearranged to look like Fig. 7 where the perturbation block in the figure includes the performance uncertainty block,  $[\Delta_p]$ , the actuation uncertainty block  $\Delta_{act}$ , additive uncertainty due modeling

errors,  $[\Delta_a]$ , and an additive uncertainty due time delays,  $[\Delta_d]$ . This time, the uncertainty block  $\Delta$  is given by

$$\Delta = \begin{bmatrix} [\Delta_p] & 0 & 0 & 0 \\ 0 & \Delta_{act} & 0 & 0 \\ 0 & 0 & [\Delta_a] & 0 \\ 0 & 0 & 0 & [\Delta_d] \end{bmatrix} \tag{27}$$

In either case, the problem reduces to finding a controller  $K$  which minimizes the infinity norm of the transfer matrix from  $\Omega_{ref}$  to  $e_L$  for all allowable  $\Delta$ 's. Using linear fraction transformation, the condition for robust performance becomes

$$\mu(F_l(P, K)(j\omega)) \leq 1 \quad \forall \omega \in [0, \infty] \tag{28}$$

where  $F_l(P, K)$  denotes the lower linear fraction transformation.

The “true” drill-string assembly vibration model corresponds to the nominal drill-string assembly plant model defined by (7), the actuator’s model defined by (16),  $W_{act}$ , and the additive uncertainties,  $[W_a]$  and  $[W_d]$  (see Fig. 2). The transfer matrices  $W_{act}$ ,  $[W_d]$  and  $[W_a]$  are assumed known, and reflect the amount of uncertainty in the model; whereas the transfer matrices  $\Delta_{act}$ ,  $[\Delta_d]$  and  $[\Delta_a]$  are assumed to be stable and unknown, but satisfy (10). The performance of the closed-loop system is evaluated by calculating the maximum singular value  $\mu$  of the weighted transfer functions from the disturbance and command input to the error output.

### 4 Simulation results

The open-loop nonlinear simulations of the drill-string system using the values listed in Table 1 are shown in Figs. 9, 10, 11 and 12. The figures clearly show that for a reference command of 10 rad/s, the disks will reach a top speed of 8.4 rad/s. Moreover, a significant amount of vibrations persists for more than 1 minute. This type of response will have a detrimental effect on the performance as well as the life of the drill string. Therefore, it is required to design a control law that will improve the performance of the drill string; i.e., less steady-state error as well as a better transient response. It is desired to have the speeds of the drill collar and the rotary table,  $\Omega_1$  and  $\Omega_2$ , reach 10 rad/s at steady state with an acceptable transient response. The control design technique used here is  $\mu$ -synthesis. This technique is linear and therefore it requires linearization of the drill-string system around

**Table 1** Values of the variables used in the simulations [19]

Variable	Value
$J_1$	374 kg m <sup>2</sup>
$J_2$	2122 kg m <sup>2</sup>
$C_1$	0–50 N m/rad
$C_2$	425 N m/rad
$K$	473 N m/rad
$T_f$	500 N m
$\alpha_1$	9.5
$\alpha$	2.2
$\beta$	35

**Fig. 9** Drill collar angular speed response without time delay using the  $\mu$ -synthesis controller

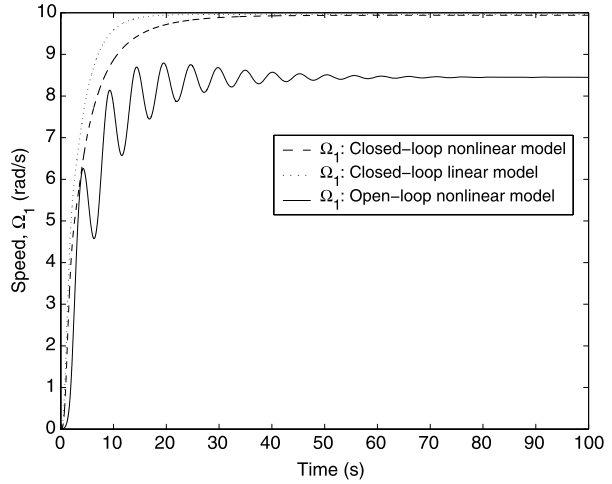
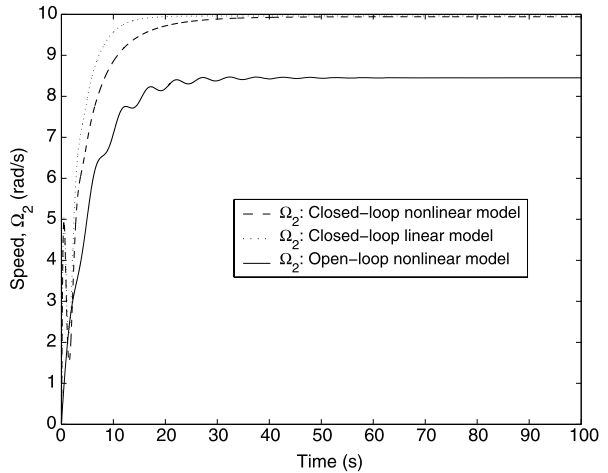


**Fig. 10** Rotary table angular speed response without time delay using the  $\mu$ -synthesis controller



a specified operating point. The drill-string system given by (5) is linearized around the operating point  $(\Omega_1, \phi, \Omega_2) = (10 \text{ rad/s}, 0, 10 \text{ rad/s})$ . The MATLAB commands **trim** and **linmod2** are used to obtain the linear model of the system. It is found that the linearized system is controllable. The difference between the linear and nonlinear model is characterized in terms of uncertainty functions as described in the previous sections. Two controllers have been designed using the  $\mu$ -synthesis control design technique. The first controller uses the drill-string model given by (7) without compensation for the sensor location and it is based on the interconnection diagram shown in Fig. 2 and the performance and uncertainty blocks defined earlier. The best controller is obtained after three D-K iterations and has 15 states, two inputs:  $\Omega_1, \Omega_2 - \Omega_{ref}$ , and one output:  $u$  as shown in Fig. 2. It was possible to reduce the number of states of the designed controller from 15 to 9 using the  $\nu$ -gap metric technique [24]. The gap between the 15-state and 9-state controllers is of the order of  $10^{-6}$ . Therefore, the difference in performance between the two controllers is virtually nil. The closed-loop system is simulated and the results are shown in Figs. 9, 10, and 11. It is clear

**Fig. 11** Twist angle response without time delay using the  $\mu$ -synthesis controller

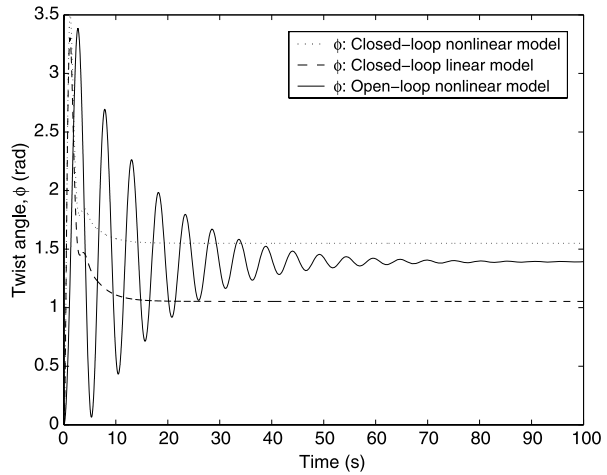
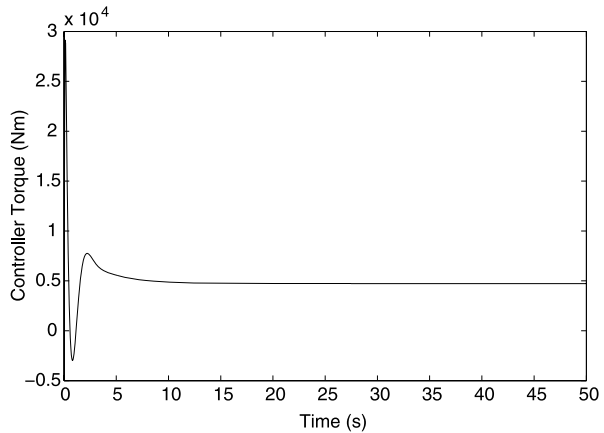


**Fig. 12**  $\mu$ -synthesis controller torque, no time delay



that the closed-loop system preserves a good performance level even under worst operating conditions. The angular speed of both the rotary table and the drill collar reach their desired value of 10 rad/s after approximately 20 seconds.

It is worth noting that the bandwidth of the closed-loop system is directly related to the cross-over frequency of the performance weight. In other words, the larger the cross-over frequency of the performance weight, the faster the closed-loop system responds. Moreover, the bandwidth of the closed-loop system is limited by the zero on the drill-string system located at 1.1 rad/s. It was possible to improve the settling time of the system; however, that was on the expense of robustness. That is, inequality (13) is no longer satisfied. This means that there exists an uncertainty matrix  $\Delta$  which destabilizes the drill-string closed-loop system [9]. On the other hand, lowering the crossover frequency of the performance weight results in a slower response, but increases the chance of achieving robust stability.

Another set of controllers were synthesized for the drill-string system with a sensor time delay included (see Fig. 3). The results of the simulations are shown in Figs. 13, 14, 15 and 16. The designed controller performed relatively well with a 2 second time delay in

**Fig. 13** Drill collar angular speed response using the  $\mu$ -synthesis controller: measurement time delay included

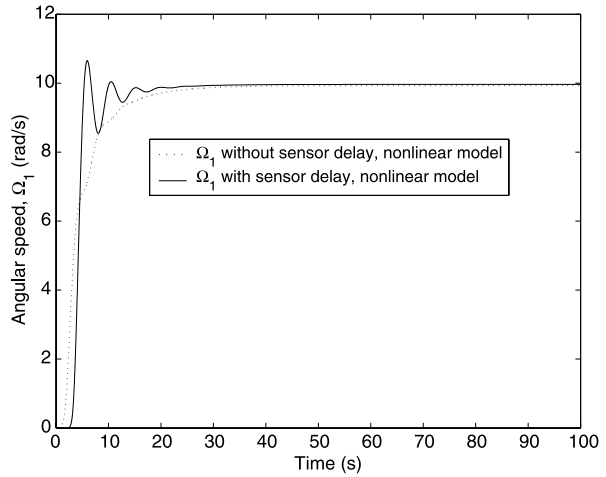
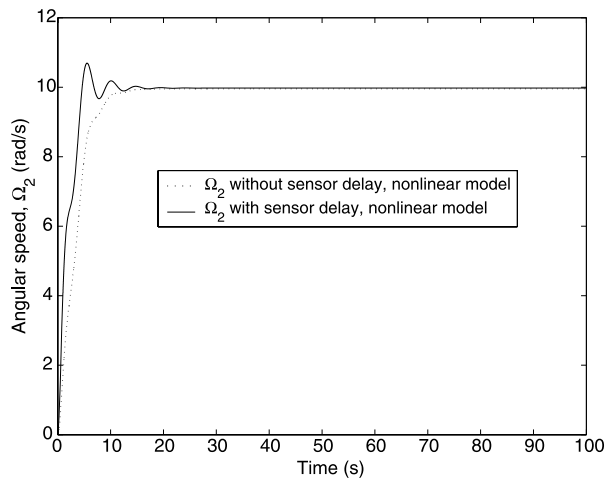


**Fig. 14** Rotary table angular speed response using the  $\mu$ -synthesis controller: measurement time delay included



the measurements. The resulting settling time is one second slower than with the previous controller.

It is worth noting that the twist angle  $\phi$  between the top and bottom disks does not go to zero no matter what performance criteria one uses (see Figs. 11 and 15). The reason for this could be explained using (5).

At steady state,  $(\dot{\Omega}_1, \dot{\phi}, \dot{\Omega}_2) = (0, 0, 0)$  and  $(\Omega_1, \phi, \Omega_2) = (10 \text{ rad/s}, \phi_c, 10 \text{ rad/s})$ . Plugging the steady-state values into (5) leads to

$$\begin{aligned}
 0 &= 10p_1 + p_2 \times \phi_c + 10p_3e^{-10\alpha} + p_4 \times \text{atan}(10\beta) \\
 0 &= p_5\phi_c + 10p_6 + p_7 + p_8\tau_c \\
 \phi_c &= \frac{10C_1}{K} + \frac{2T_l}{\pi K} (10\alpha_1 e^{-10\alpha} + \text{atan}(10\beta)) \neq 0 \\
 \tau_c &= 10C_1 + \frac{2T_l}{\pi} (10\alpha_1 e^{-10\alpha} + \text{atan}(10\beta)) \neq 0
 \end{aligned}$$

**Fig. 15** Twist angle response with time delay using the  $\mu$ -synthesis controller: measurement time delay included

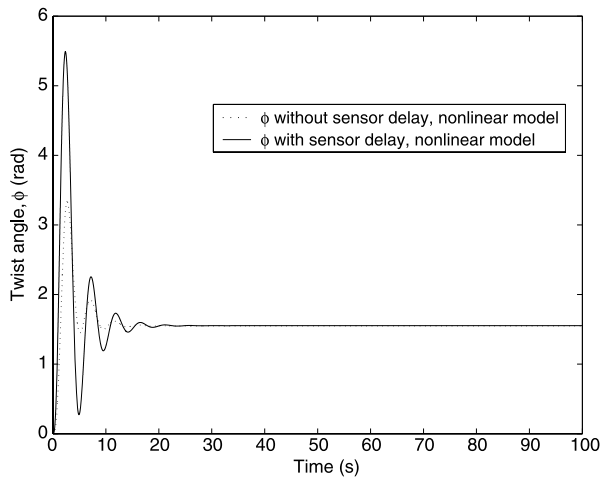
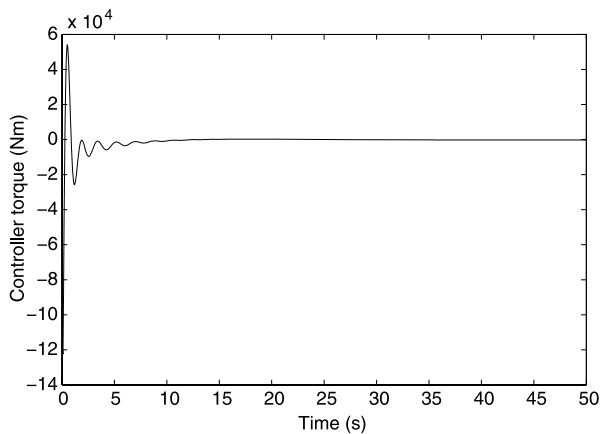


**Fig. 16**  $\mu$ -synthesis controller torque, with time delay



Although the steady-state twist angle  $\phi$  does not go to zero, its vibration has been greatly reduced.

## 5 Concluding remarks

Torsional vibrations of drill strings caused by stick-slip friction are detrimental to the whole drilling process. They can lead to excessive loadings resulting in equipment wear, joint failure, or damage of the drill-bit. Because of the energy lost to torsional vibrations, the application of a constant rotary speed at the surface does not necessarily translate to a constant rotational speed of the drill-bit. Therefore, it is necessary to suppress the vibrations of drill strings to improve their life and performance. Robust controllers have been designed using the  $\mu$ -synthesis technique and applied to the drill-string system to suppress its stick-slip induced vibrations. The controllers are robust to unmodeled nonlinearities, high frequency dynamics, actuator uncertainties, and noise. The designed controllers performed well even under extreme uncertainty conditions and with measurement time delay. It is worth noting

that if more degrees of freedom are included in the dynamic system such as bit bounce and lateral motion, the control problem becomes more challenging and might not lead to good performance. Many other control techniques are available in the literature such as switching and passivity based control techniques. Even these methods do not guarantee good performance if more than two degrees of freedom are un-actuated. Currently, we are working on developing a 4 degree-of-freedom model for a drill-string system. The control technique proposed here will be extended to the 4 degree-of-freedom model and the results will be made available in due time. The proposed control scheme can be easily extended to the 4 degree-of-freedom model by augmenting the weighting matrices to account for the extra degrees of freedom. However, the performance specs may have to be relaxed to increase the chances of success of the control technique presented in this paper.

## References

1. Abdulgalil, F., Siguerdidjane, H.: Backstepping design for controlling rotary drilling system. In: Proceedings of 2005 IEEE Conference on Control Applications, pp. 120–124 (2005)
2. Abdulgalil, F., Siguerdidjane, H.: PID based on sliding mode control for rotary drilling system. In: Proceedings of EUROCON 2005 Conference, pp. 262–265 (2005)
3. Al-Hiddabi, S.A., Samanta, B., Seibi, A.: Nonlinear control of torsional and bending vibrations of oil well drill strings. *J. Sound Vib.* **265**, 401–415 (2003)
4. Balas, G.J., Doyle, J.C., Glover, K., Packard, A., Smith, R.:  $\mu$  Analysis and Synthesis Toolbox. MUSYN and the Mathworks Inc. (1995)
5. Brett, J.F.: The genesis of torsional drill string vibrations. In: SPE Drilling Engineering, pp. 168–174 (1992)
6. Canudas-de-Wit, C., Corchero, M.A., Rubio, F.R., Navarro-Lopez, E.: D-OSKIL: a new mechanism for suppressing stick-slip in oil well drill strings. In: 44th IEEE Conference on Decision and Control and 2005 European Control Conference, CDC-ECC '05, pp. 8260–8265 (2005)
7. Chevallier, A.: Nonlinear stochastic drilling vibrations. PhD Thesis, Rice University, Department of Mechanical Engineering and Material Science, Houston, Texas (2000)
8. Christoforou, A.P., Yigit, A.S.: Fully coupled vibrations of actively controlled drillstrings. *J. Sound Vib.* **267**, 1029–1045 (2003)
9. Doyle, J.C.: Analysis of feedback systems with structured uncertainties. *Proc. IEEE, D* **129**, 242–250 (1982)
10. Hernandez-Suarez, R., Puebla, H., Aguilar-Lopez, R., Hernandez-Martinez, E.: An integral high-order sliding mode control approach for stick-slip. *J. Petroleum Sci. Technol.* **27**, 788–800 (2009)
11. Jansen, J.D., van den Steen, L.: Active damping of self-excited torsional vibrations in oil well drill strings. *J. Sound Vib.* **179**(4), 647–668 (1995)
12. Karkoub, M.A.: Robust control of a flexible slider-crank mechanism using  $\mu$ -synthesis. *Mechatronics J.* **10**(6), 649–668 (2000)
13. Leine, R.I., van Campen, D.H., Keultjes, W.J.G.: Stick-slip whirl interaction in drill string dynamics. *J. Vib. Acoust.* **124**, 209–220 (2002)
14. Mihajlovic, N., Van Veggel, A.A., Van de Wouw, N., Nijmeijer, H.: Analysis of friction-induced limit cycling in an experimental drill-string system. *ASME J. Dyn. Syst. Meas. Control* **126**, 709–720 (2004)
15. Mihajlovic, N., Van de Wouw, N., Rosielle, P.C.J.N., Nijmeijer, H.: Interaction between torsional and lateral vibrations in flexible rotor systems with discontinuous friction. *Non. Dyn.*, author pre-print (2007)
16. Navarro-Lopez, E.M., Suarez, R.: Practical approach to modeling and controlling stick-slip oscillations in oil well drill strings. In: Proceedings of the 2004 IEEE International Conference on Control Applications, vol. 2, pp. 1454–1460 (2004)
17. Pavone, D.R., Desplans, J.P.: Application of high sampling rate downhole measurements for analysis and cure of stick-slip in drilling, SPE 28324. Paper presented at the SPE 69th Annual Technical Conference and Exhibition held in New Orleans, 25–28 September 1994
18. Placido, J.C.R., Santos, H.M.R., Galeano, Y.D.: Drill string vibration and wellbore instability. *J. Energy Resour. Technol.* **124** (2002)
19. Serrarens, A.F.A.:  $H_\infty$  control as applied to torsional drill-string dynamics. MSc. thesis, Eindhoven University of Technology, The Netherlands (2002)
20. Smit, A.T.: Using of optimal control techniques to dampen torsional drill strings vibrations. PhD thesis, University of Twente (1999)



21. Spanos, P.D., Chevallier, A.M., Politis, N.P., Payne, M.L.: Oil and gas well drilling: a vibrations perspective. *The Shock Vib. Dig.* **35**, 85–103 (2003)
22. Tucker, R.W., Wang, C.: On the effective control of torsional vibrations in drilling systems. *J. Sound Vib.* **224**(1), 101–122 (1999)
23. Van den Steen, L.: Suppressing stick-slip-induced drill string oscillations: a hyperstability approach. Ph.D. Thesis, University of Twente, Faculty of Electrical Engineering and Applied Physics (1997)
24. Vinnecombe, G.: Measuring robustness of feedback systems. PhD dissertation, Department of Engineering, Cambridge (1993)